Microbubble skin friction reduction on an axisymmetric body

S. Deutsch and J. Castano[a)]
Applied Research Laboratory, The Pennsylvania State University, Post Office Box 30, State College, Pennsylvania 16804

(Received 3 October 1985; accepted 23 July 1986)

A reduction in skin friction drag is shown when gas is introduced into the liquid turbulent boundary layer of a submerged axisymmetric body. The 89 mm diameter, 632 mm long body has a cylindrical balance 273 mm long. Free stream speeds in the 305 mm diameter tunnel are as high as 17 m/sec, giving length Reynolds number of up to 10 million. In general, skin friction reduction is shown to increase with increasing free stream speed. At high speeds, helium injection is shown to be more effective at reducing skin friction than is air injection. Maximum skin friction reduction is near 80%—a value in good agreement with the maximum value observed in the flat plate work of Madavan *et al.* [Phys. Fluids **27**, 356 (1984)]. While maximum skin friction reduction was found at a free stream speed of 5 m/sec for the flat plate geometry, maximum skin friction reduction was at a free stream speed of 17 m/sec for the axisymmetric geometry.

I. INTRODUCTION

The injection of a gas (to form microbubbles) into a liquid turbulent boundary layer has been shown, in several studies,[1–8] to reduce drag. For the most part, these studies have looked at the skin friction reduction that might be obtained in a flat plate geometry.[1–7] The drag reduction mechanism is not very well understood; only two rudimentary analytical/computational studies[9,10] have been attempted. While the key to a fundamental understanding of the phenomenon would appear to lie in an understanding of bubble dynamics in a boundary layer flow, it seems plausible from the computational work,[9] when taken in concert with some bubble concentration profile measurements,[4–6] that the bubbles provide a mechanism for increasing the kinematic viscosity near the buffer region, thereby destroying some of the turbulent production. A similar mechanism has been postulated for the polymer drag reduction phenomenon.[11]

In the current study, the series of microbubble skin friction reduction experiments is extended to a more practical, axisymmetric geometry. The scope of the study is very much like that undertaken by Madavan *et al.* (MDM).[1] Therefore, before proceeding, we shall present a summary of their results. A more detailed review of all of the earlier microbubble work has been given by Merkle and Deutsch.[12]

The most recent series of experiments in microbubble drag reduction were performed by Madavan *et al.*[1–3] in a 508×114 mm rectangular test section 762 mm long. The flat plate employed was mounted flush to a tunnel wall in a 279×533 mm long slot intended for a window. A 102 mm wide by 178 mm long porous section was placed upstream of a force balance 102×254 mm long. For the initial tests, the porous section was constructed from a sintered stainless steel filter material with a nominal pore size of 5 μ. Both in the MDM tests and the current axisymmetric tests described here, this pore size actually refers to the largest particle size that can pass through the filter material. MDM[3] have shown that pore size is not a primary variable. The orientation of the plate with respect to gravity was varied by rotating the test section. Tests were made with the plate above, below, and alongside the microbubble filled turbulent boundary layer.

Mean velocity and turbulent intensity profiles were measured at three streamwise locations on the drag balance section in the undisturbed boundary layer. The profiles appeared to be fully developed at speeds above 5 m/sec. Length Reynolds numbers, based on a fictitious boundary layer origin, deduced from the velocity profiles, were between 2.2 and 10.6 million. Static pressure measurements showed that the pressure varied by no more than 0.8% of the dynamic head over the length of the test plate. When taken together, the velocity profiles and pressure measurements established the flow as being reasonably close to a zero pressure gradient turbulent boundary layer.

Integrated skin friction on the floating element force balance was measured at free-stream speeds of 4.2–17.4 m/sec. The results show skin friction reductions ranging from 50%–80% (depending on plate orientation) at a maximum air flow rate near 5×10^{-3} m^3/sec. The largest reductions occurred for the plate on top case where buoyancy tended to keep the bubbles in the boundary layer. In contrast to the results of some earlier Soviet work,[4,6,7] maximum drag reduction was found at the lowest speed tested. This would appear to indicate that buoyancy was not a major factor in the MDM tests, but rather that the drag reduction was limited by the availability of gas at the higher tunnel speeds. Note that the work of MDM[1–3] and the Soviet work[4,6,7] complement rather than contradict each other. Some unpublished work by MDM indicates that the drag reduction decreases, for the plate on bottom configuration, as the free stream speed is reduced below about 4 m/sec and buoyant effects become large. MDM[1] also performed some experiments with helium. Helium injection was found to give the same reduction as air injection, suggesting that the density of the gas was not an important variable. We note that these density variation experiments were performed only for a plate

[a)] Present address: Naval Underwater Systems Center, Newport, Rhode Island 02841.

 0031-9171/86/113590-08$01.90

on top configuration in which buoyant effects might not have been as important as for the plate on bottom or the plate alongside geometries.

In the initial MDM experiments,[1] the local skin friction was measured by a surface mounted hot film probe located 51 mm from the trailing edge of the porous material. For the plate on the bottom orientation, local reductions of nearly 90% were observed. MDM reported that oscilloscope traces of the surface mounted hot film probe output signal showed no sign of bubble impingement (as opposed to a hot film probe in the boundary layer, say). This confirmed the concentration measurements made by Bogdevich and Maliuga[6] that indicated that the bubbles were not present in the region (sublayer) closest to the wall. This apparent lack of bubbles in the very near wall region is important, if one is to believe that a major mechanism for the bubble drag reduction is the selective increase of kinematic viscosity (in the buffer region).[9]

A second series of experiments, employing an array of hot film probes on the balance was also conducted by MDM.[2] Using this array they were able to show that substantial drag reduction persisted for as much as 60 to 70 boundary layer thicknesses downstream of the injection section. The loss of some of the turbulent production scales was confirmed through spectral measurements; the similarity of the shear stress spectra for microbubble boundary layers and polymer boundary layers[13] was quite striking.

In the current experiment, skin friction drag measurements are extended to an axisymmetric body. To facilitate comparison between the current study and the work of MDM,[1] some boundary layer parameters are presented for each in Table I. We note that these are the only two microbubble studies for which details of the undisturbed boundary layer are available. The lack of boundary layer measurements in the other reported studies makes interpretation and comparison of the data difficult.

TABLE I. Comparison of LDA data.

MDM flat plate (from Refs. 1–3)				
Location[a]	u_∞ (m/sec)	R_θ	u^+ (m/sec)	y at $y^+ = 5$ (μm)
272	4.68	3 372	0.195	25.6
	10.90	7 358	0.423	11.8
374	4.75	4 215	0.190	26.3
	10.30	8 862	0.392	12.7
454	4.78	5 127	0.188	26.6
	10.47	10 627	0.392	12.7
Axisymmetric body				
Location[b]	u_∞ (m/sec)	R_θ	u^+ (m/sec)	y at $y^+ = 5$ (μm)
155	5.26	2 635	0.21	23.8
	10.71	5 062	0.405	12.3
	16.94	8 837	0.607	8.24
277	5.25	3 491	0.21	23.8
	10.77	6 764	0.406	12.3
	16.86	10 144	0.617	8.10
403	5.30	3 775	0.210	23.8
	10.90	8 191	0.413	12.11
	16.88	14 197	0.594	8.42

[a] From virtual origin.
[b] From trip wire.

II. FACILITIES AND PROCEDURES

The current experiment was run in the 305 mm diameter tunnel at the Applied Research Laboratory of The Pennsylvania State University. This tunnel, but with the rectangular section in place, was previously described by MDM.[1] Tunnel velocity, pressure, and gas injection flow rates were controlled manually. The tunnel has a bypass mechanism to purge the water of gas accumulation. In general, this allowed for long periods of continuous gas injection without serious fluctuations in the tunnel speed and pressure. Data acquisition and reduction were accomplished through an on-line VAX 11/780 computer system.

Figure 1 shows the 89 mm diameter axisymmetric model. The overall length of the model is 632 mm. An isolated cylindrical section with an extremely stiff shear member serves as a force balance to measure the skin friction. The balance is 273 mm long with gaps of 0.127 and 0.254 mm located at axial distances of 196 and 469 mm from the nose, respectively. Because of the stiffness of the shear member, the gaps could be carefully aligned to minimize the risk of pressure effects. Maximum balance displacement was estimated, theoretically, to be no more than 2.5 μ. This extremely small balance displacement assures that the gaps will remain aligned over the entire range of tunnel velocities employed. A 6.35 mm long and 5.17 mm thick, cylindrical, sintered porous plastic section, with a nominal pore size of 5 μ, was used to inject the gas at a distance of 146.5 mm from the nose. Note that the length of the injection section was much shorter than the 178 mm long injection section used by MDM. There was some initial concern that buoyant effects might serve, in this cylindrical geometry, to drive the gas flow through only the upper part of the cylindrical injection section. To work around this, the gas was first directed to the bottom of an internal cylindrical plenum chamber through a set of adjustable partitions. In this way we hoped that the gas would have a tendency to enter the filter material at the bottom of the model, and this tendency would help compensate for any buoyant effects. Visual inspection of the gas in-

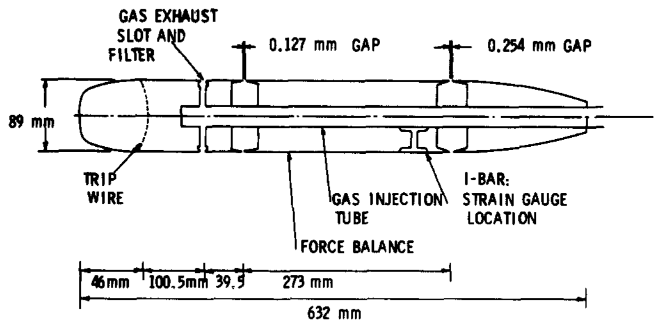

FIG. 1. Axisymmetric skin friction model.

jection, which was possible through two sides and the top of the tunnel, showed no evidence of a bubble cloud asymmetry at the site of the injection.

A steel wire, 0.35 mm in diameter, was placed 46 mm from the leading edge in an effort to trip the boundary layer and help ensure a fully developed turbulent boundary layer over the measuring section. A 200 mm long sting mount held the model in the center of the test section; two 127 mm long streamlined struts inclined at 45 deg from the sting were attached to the lower tunnel wall immediately behind the model. Identical dummy struts were placed symmetrically opposite the support struts to preserve flow symmetry.

The balance employed a strain-gauged shear member to infer the integrated skin friction on the surface. The balance was dry calibrated in place in the test section using a radially centered pulley and incremental weights. The balance showed excellent linearity. Several of the calibrations were made with air injection and showed that injection had no effect on the measured drag. Throughout the test program the response of the balance was checked against tunnel speed for consistency and no measurable drift was noted.

Gas injection flow rates were measured with a rotameter. The rotameter was calibrated to measure air flow rates at standard atmospheric pressure and temperature. Gas flow rates were corrected for the actual injection pressure and for the density of the injected gas. Gas temperature was not measured during injection, but subsequent bench tests indicated that both gases were injected at near room temperature for the range of pressures and flow rates employed.

The gas volume flow rate, the free stream velocity, and the type of gas (air or helium) were systematically varied to determine the influence each had on the skin friction drag. The test procedure was as follows. First, no gas "reference" drag tests provided skin friction drag as a function of the mean flow speed over the range 0–17 m/sec. The tunnel speed was then fixed at one of the four (4.6, 7.6, 10.7, or 16.8 m/sec) test velocities. At each of these velocities the skin friction drag was measured against gas flow rate, as the gas flow rate was incrementally stepped from zero to maximum and then back to zero. The skin friction drag was then normalized by the no gas reference drag data at the given velocity and placed in "bins" as a function of gas flow rate. Multiple runs were used to provide statistics on the data. A Student T-test was used to calculate 95% confidence levels for the data in each bin. In this way we were able to construct one curve of normalized drag reduction data against gas flow rate for each gas at each of the tunnel test velocities.

Two additional points are worth noting. First, the no gas reference drag tests were conducted both before and after each gas injection test. Significant variation between tests would be grounds for ignoring the entire data set. No such variations were observed. Second, the injection of gas causes a drop in mean velocity, which is corrected manually. As in the MDM[1] work, we found that fluctuations caused by the continual injection of gas and subsequent correction could be kept very small ($\pm 1\%$), so that it was not necessary to correct the data for a fluctuating velocity.

To help define the undisturbed flow field both velocity profiles and the test section static pressure distribution were measured. Laser Doppler velocimetry (LDV) was used to measure the velocity profiles at three locations (155, 277, and 403 mm downstream of the trip wire) on the balance to determine the characteristics of the undisturbed boundary layer. As these high unit Reynolds number boundary layers are extremely thin (prohibiting hot film probes) and optical access to the tunnel is limited, it was not possible to measure the boundary layer at the gas injection filter. Such information would be useful in attempting to discern the effect of bubble injection on the state of the boundary layer, should the boundary layer be transitional. Although not attempted in the current study, a flush-mounted hot film probe, mounted just downstream of the injection filter, would probably be able to resolve this question.

The LDV was composed of a Spectra-Physics 8 W argon–ion laser and power supply, and TSI optics consisting of a $3.75\times$ beam expander, a 460 mm transmitting lens, and a model 1980 counter processor. A trace of 1.5 μ silicon-carbide particles was added to the tunnel as seed. Data reduction was through the VAX 11/780 computer.

As in MDM,[1] to achieve a reasonable LDV signal very close to the wall, the entire optical package was tilted at an angle of 8 deg to the horizontal. A consistent reference point in the boundary layer was determined by focusing the LDV control volume on the body. Experience with this technique suggests a repeatability of some 50 μ in determining the initial location.

The single component, dual beam system was operated in the backscatter mode. The turbulence intensity dictated the number of samples that was taken at each point in the boundary layer; 200 points for turbulence intensities below 5%, 500 samples for turbulence intensities below 10%, and 1000 samples for turbulence intensities above 10%. The number of samples was chosen, in each case, to insure reasonable repeatability of the mean velocity and the turbulence intensity.

The static pressure distribution along the test section wall was measured using a bank of individual pressure transducers. The pressure was measured at six axial locations, 104 mm apart along the wall, with the first tap positioned 109.5 mm downstream of the nose. In order to check for axial symmetry, a pressure reading was taken from each of the four quadrants of the circular test section at each of the axial locations. The pressure tap in each quadrant was lined up circumferentially with the support and dummy support struts. Surveys were taken at 20 to 30 air injection rates (to 3.6×10^{-3} m^3/sec) to test for possible pressure variations or flow asymmetry with injection.

It should be noted that the free stream velocity at the model was calculated from measurements made by differencing the settling section pressure against the static pressure at the second tap location in the test section (213.5 mm from the nose). Approach velocities were then some 10% lower.

III. RESULTS

The no gas injection, skin friction coefficient (based on the surface area of the balance) is shown as a function of

Reynolds number (based on the maximum model diameter) and tunnel speed in Fig. 2. The test data presented span the entire period of the experiment and are characteristic of data taken for both increasing and decreasing tunnel speed. With the exception of the data taken at the lowest speeds, at which deviations between runs are as high as 10%, repeatability is excellent. The low speed deviations are characteristic of drag balance data and are basically a result of the need to cover a very large range of forces (roughly proportional to the velocity squared). A consequence of this sensitivity at low speeds can be seen in the relatively large error bands associated with the skin friction data taken at a free stream speed of 4.6 m/sec (cf. Fig. 6), as opposed to the error bands for the data taken at the higher speeds (cf. Figs. 7–9).

LDV surveys of the boundary layer, at 155, 277, and 403 mm downstream of the trip wire, were taken at free stream speeds of 5.25, 10.8, and 16.88 m/sec. The shear velocity was estimated from a "Clauser plot"-like technique. The shear velocity may also, of course, be roughly estimated from the drag balance data. Comparisons between the results of these two measuring techniques agreed to within 10%. The shear velocity data is also in good agreement with classical flat plate correlations. Some characteristic boundary layer profiles, for a range of momentum thickness Reynolds numbers are shown in inner variables in Fig. 3. The solid line is the law of the wall.

Following Purtell *et al.*[14] we test for underdevelopment of the boundary layer by examining, at each of the measurement locations, a plot (see Fig. 4) of u/U_∞ vs y/δ^*, with δ^* the local displacement thickness. At each of the speeds, the curves collapse reasonably well, indicating that the profiles are fully developed, even at 5 m/sec, at the location of the balance section. Once again, boundary layer profiles at the injection site would be of value.

Some comparisons with the MDM[1] boundary layer data are shown in Table I. Note that if the data are compared at the same distance from their virtual origins (in the case of the axisymmetric body this is assumed to be at the trip wire), and at the same free stream speed, both the inner and the outer scales are fairly close. For the MDM[1] data, however, the balance section is some 100 mm further downstream of its origin than is the axisymmetric balance section. Recall, in this regard, that the MDM boundary layer is being grown, without a trip, on one wall of the water tunnel, while the

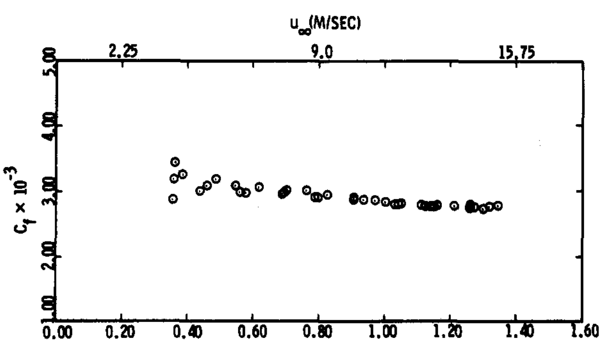

FIG. 2. Skin friction drag coefficient versus maximum diameter Reynolds number.

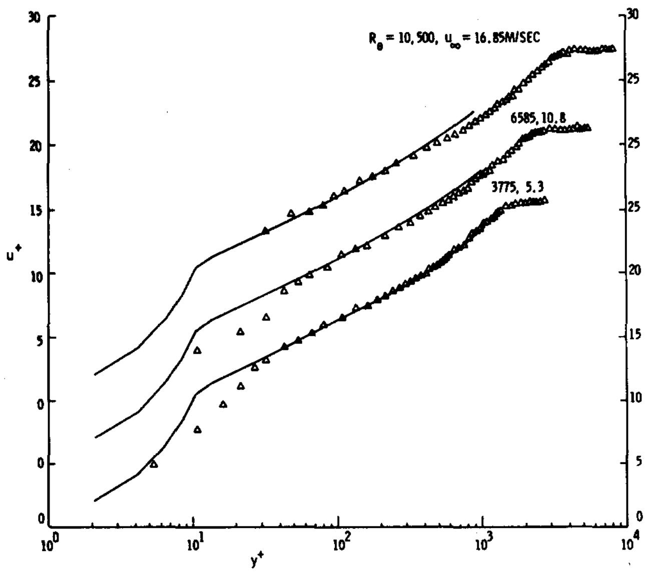

FIG. 3. Some typical boundary layer velocity profiles on the balance section in inner variables.

axisymmetric boundary layer is grown on a model mounted in the tunnel and is tripped. On their respective balance sections then, the MDM boundary layers are some 40% larger than those of the axisymmetric model. Inner scales are still quite close.

As noted earlier, the symmetry of the flow during air injection was checked by comparing the wall static pressure distribution taken along the four quadrants of the tunnel test section, at six axial locations. A typical normalized velocity distribution is given as a function of the pressure tap axial location in Fig. 5. For convenience in interpreting the plot, the location of the balance section is included in the figure. Note that the flow exhibits excellent axial symmetry both with and without gas injection. In all cases the velocity is reasonably constant across the balance section, indicating the presence of a zero pressure gradient flow—a result that does not change with gas injection. The strong decrease in velocity at the last pressure tap is caused by the increased flow area as the tail of the body is approached.

The skin friction reduction data are presented for free stream velocities of 4.6, 7.6, 10.7, and 16.8 m/sec in Figs. 6–

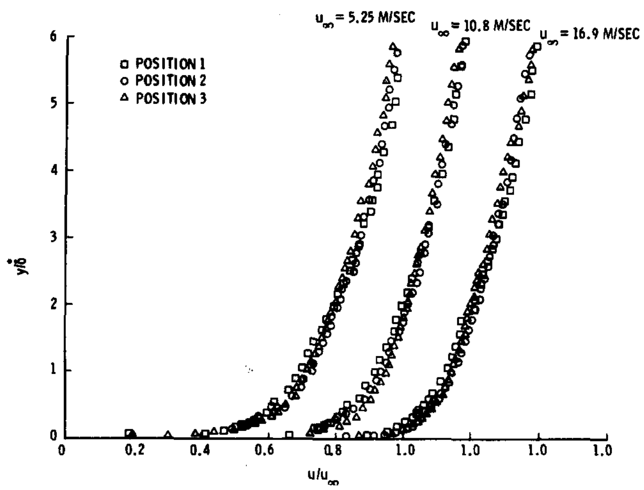

FIG. 4. Balance section velocity profiles in outer variables.

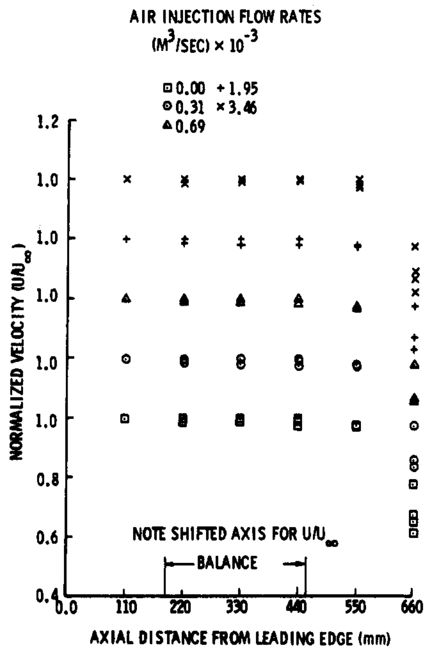

FIG. 5. Normalized velocity distribution determined from static pressure measurements.

9. Mean drag reduction data are presented as the ratio of skin friction drag to the no gas injection skin friction drag, against the gas volumetric flow rate. Each data point on the figure is the average value over several independent tests. Also shown in the figures are 95% confidence levels as determined by a Student T-test. Confidence bands are generally wider for the helium injection data as fewer overall tests were run because of a lack of gas availability for the bottled helium. The range of gas volumetric flow rates employed in the MDM work is shown for convenience on the figures.

The data taken at 4.6 m/sec (see Fig. 6) shows that the drag, at the lowest gas flow rates, initially increases with the gas injection. This suggests that the injection may be hastening the transition of an underdeveloped boundary layer at this low speed. Boundary layer data at the injection location is not available to check this hypothesis. A maximum drag reduction, of 20% for air and 15% for helium, occurs at gas flow rates between 1.5 and 2.5×10^{-3} m^3/sec. Increasing the gas flow rate further leads to substantially smaller reductions for both the air and the helium injection. At the largest flow rates, the helium data indicate skin friction ratios near one. Photographs taken under these conditions show that the bubbles have in fact left the boundary layer region. The helium results have apparently returned to their undisturbed drag value, within the scatter, because buoyancy effects (stronger at higher gas flow rates because of the larger bubble sizes[14]) have made the bubbles ineffective as drag reducers. The effect of buoyancy on the denser air is not as strong.

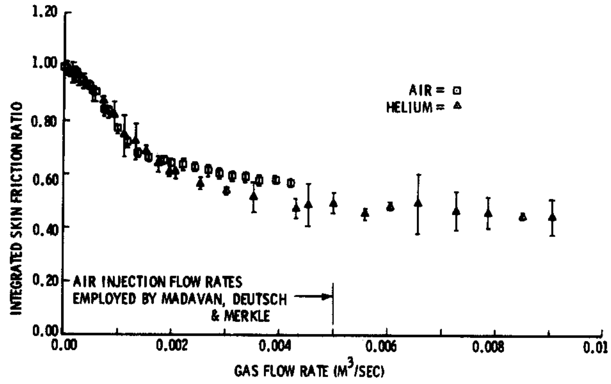

FIG. 7. Drag reduction at 7.6 m/sec.

Drag reduction data taken at a mean speed of 7.6 m/sec are shown in Fig. 7. Here the initial drag overshoot is absent, suggesting that the undisturbed boundary layer is fully developed at this speed. The drag reduction for both the helium and air is roughly the same, in agreement with the work of MDM.[1] Note, however, that the maximum drag reduction at this speed is larger than at 4.6 m/sec. This would seem to indicate that strong buoyant effects are absent at and above speeds of 7.6 m/sec.

The drag reduction data for free stream speeds of both 10.7 and 16.8 m/sec are quite similar. At both speeds, the drag reduction seems to be (slowly) leveling off at high gas flow rates. Hughes *et al.*[15] predicted that initial bubble size would grow proportionally with $\sqrt{Q}$ for constant tunnel velocity. One might speculate that bubble sizes would likely remain larger at high gas flow rates as the small scale turbulence, most effective at breaking them down, would have been destroyed by the drag reduction mechanism. The larger bubbles produced at the higher gas flow rates then (because they are influenced more by buoyancy) are perhaps less effective at reducing drag. The data taken at 10.7 m/sec show large reductions in skin friction for both air and helium injec-

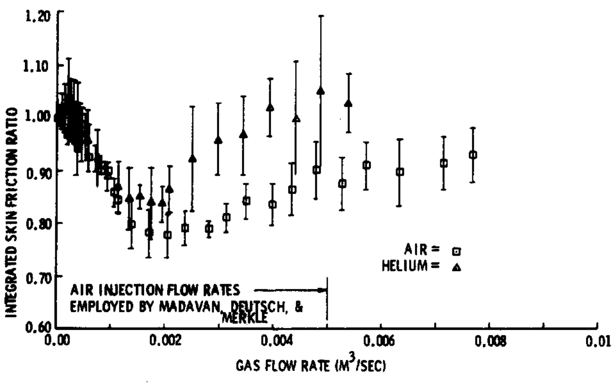

FIG. 6. Drag reduction at 4.6 m/sec.

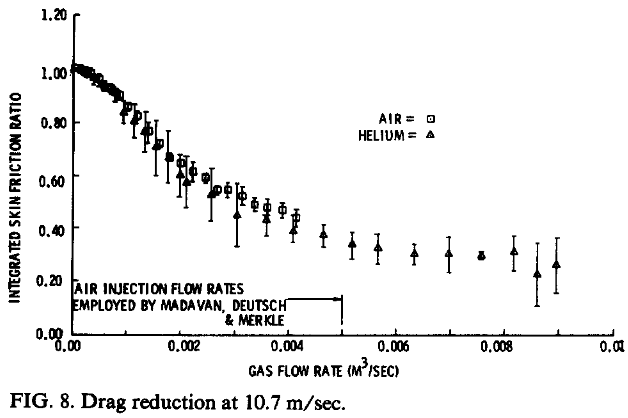

FIG. 8. Drag reduction at 10.7 m/sec.

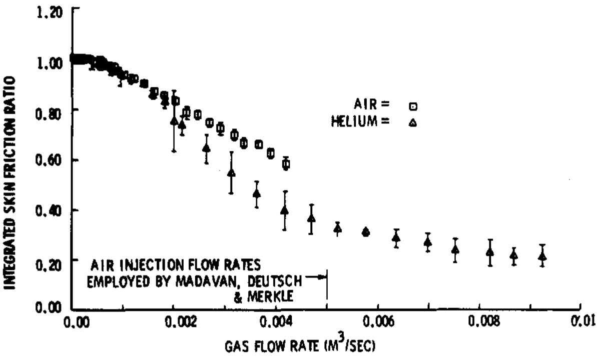

FIG. 9. Drag reduction at 16.8 m/sec.

tion; the maximum drag reduction for air injection occurs at this tunnel speed. Larger air flow rates than were available would be needed to see if the reduction with air injection has the same high gas flow rate asymptote as the helium injection at a free stream speed of 10.7 m/sec. At a tunnel speed of 16.8 m/sec, helium injection is clearly a more effective skin friction reducer than is air injection. At an air flow rate of 4.0×10^{-3} m^3/sec, for example, a skin friction drag reduction of about 60% is obtained with helium as opposed to 40% for air. This result, although intriguing, is not well understood. In particular, although the density difference between the gases is the leading candidate for the difference in drag reduction, other properties, such as gas solubility may play a role. We note here, that in some unpublished results we have shown that carbon dioxide is ineffective in reducing drag—a result that is difficult to attribute entirely to the higher density of carbon dioxide relative to air or helium. We might note further that neither the simple computational work of MDM,[9] nor the analytical work of Legner[10] provides any mechanism for describing these differences. Clearly more analytical and experimental work is needed.

In Fig. 10, we present a comparison of the integrated skin friction drag ratio against the dimensional gas flow rate for both the MDM and the axisymmetric geometries. Note that the flat plate data presented in Fig. 10 has been taken from the more extensive data set of Madavan.[16] Two things are quite striking. First, is the large difference in the results—which are apparently buoyancy related—between the two geometries at the lowest speed. Visual evidence is that the bubbles have risen off the bottom of the balance section of the axisymmetric body at this low speed. Drag reduction, however, is quite effective (most effective for the plate on top) for the flat plate at this speed. Second, is just how similar the drag reduction results are, at the higher speeds, for both geometries. A reviewer has suggested that buoyancy effects might average out in the axisymmetric geometry. This seems to be the case at the single speed near 11 m/sec, but clearly the influence of buoyancy is generally more complicated.

The results of Fig. 10 illustrate the differing effect of free stream speed on the drag reduction for the two geometries. While for the flat plate the drag reduction was most effective at 5 m/sec, bubble drag reduction was most effective near 11 m/sec (air) or 17 m/sec (helium) for the axisymmetric geometry. Clearly some theoretical insight into the dynamics of the bubble cloud in a turbulent boundary layer would be of great use in resolving these differences. In this regard, we should note that Legner[17] has outlined a theory, based on bubble sizes, which may help to physically explain the drag reduction versus speed results obtained in the MDM[1] and the Soviet[4,6,7] studies. Legner postulates that to be most effective the bubble sizes should be in a region in which they are likely to coalesce. An attempt to fit the current results into Legner's theoretical framework would be of value.

IV. CONCLUSION

The injection of gas to form microbubbles in a liquid turbulent boundary layer has been shown, through a series of water tunnel tests, to be effective in reducing skin friction drag on an axisymmetric body. Both helium and air were used in the experiments.

Injection of helium (at high speeds) and air (at moderate speeds) produced large skin friction drag reductions of roughly 80% and 55%, respectively. The observation that the amount of drag reduction was a function of gas type was unexpected since earlier observations by MDM[1] using air and helium injection suggested that this was not the case. Additional studies in the simpler flat plate geometry appear to be warranted.

The skin friction drag reduction increased monotonically with the gas flow rate at all but the lowest tunnel velocity tested. At this lowest speed, of 4.6 m/sec, the drag data show both an initial increase with gas injection and an optimal gas flow rate above which the drag values begin to rise. The initial drag rise is possibly due to a bubble induced change in the transitional boundary layer at 4.6 m/sec.

Certainly from a practical standpoint, the observation that maximum drag reduction, while equivalent to the flat plate value, is found at 17 m/sec rather than at 5 m/sec is a major result. Based on simple extrapolation of the flat plate studies,[1–7] the observation of larger drag reduction at the higher tunnel speeds is an unexpected result. The differing results are apparently due to the differing influence of buoyancy in each geometry. It appears that higher free stream velocities are needed in the axisymmetric geometry to sustain effective concentrations of bubbles in the boundary layer.

It is apparent from all the experiments done to date that large reductions in skin friction[1–7] and total drag[8] may be obtained by using gas injection in a liquid turbulent boundary layer, provided that a sufficient concentration of (sufficiently small) bubbles can be maintained in the near wall region. The extrapolation of these results to practical geometries at practical Reynolds number, as well as calculations of the gas flow rate necessary, is very much dependent on the dynamics of the bubbles in these situations. Information on bubble trajectories and bubble sizes (and the evolution of sizes in the changing turbulent field) are necessary. The theoretical framework to formulate such a view of bubble dynamics is currently lacking. Experiments, in which the influence of various parameters (e.g., pressure gradient, density) on the drag reduction is catalogued, or in which the phenomenon is examined in boundary layers with widely

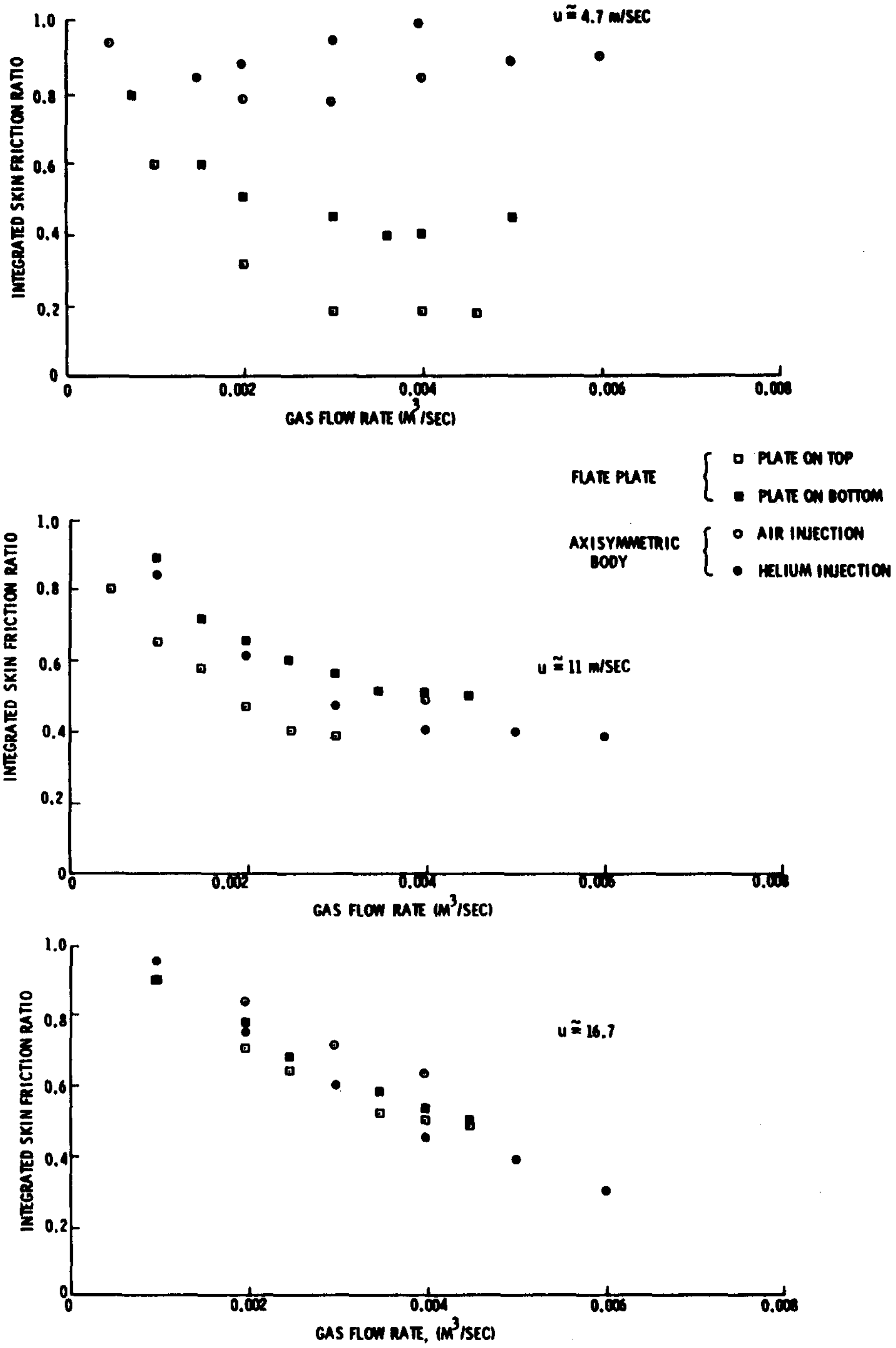

FIG. 10. Some skin friction drag comparisons between the flat plate work of MDM[1] and the current axisymmetric body study.

different inner or outer flow parameters, should be useful in providing insight for theoretical models.

ACKNOWLEDGMENTS

Professor George B. Gurney designed the force balance. Discussions between the authors and Professor Charles L. Merkle of the Mechanical Engineering Department at Penn State were very helpful.

This work was supported by the Naval Sea Systems command under Contract N00024-79-6-60403.

[1]N. K. Madavan, S. Deutsch, and C. L. Merkle, Phys. Fluids **27**, 356 (1984).

[2]N. K. Madavan, S. Deutsch, and C. L. Merkle, J. Fluid Mech. **156**, 237 (1985).

[3]N. K. Madavan, S. Deutsch, and C. L. Merkle, AIAA Publ. 84-0348, 1984.

[4]G. S. Migirenko and A. R. Evseev, *Problems of Thermophysics and Physical Hydrodynamics* (Nauka, Novosibirsk, 1974) (in Russian).

[5]Yu. N. Dubnishchev, E. R. Evseev, V. S. Sobolev, and E. N. Utkin, J. Appl. Mech. Tech. Phys. **16**, 114 (1975).

[6]V. G. Bogdevich and A. G. Maluga, in *Investigations of Boundary Layer Control*, edited by S. S. Kutateladze and G. S. Migirenko (Thermophysics Institute, Novosibirsk, 1976), p. 62 (in Russian).

[7]V. G. Bugdevich and A. R. Evseev, in Ref. 6, p. 49.

[8]M. E. McCormick and R. Bhattacharyya, Nav. Eng. J. **85**, 11 (1973).

[9]N. K. Madavan, S. Deutsch, and C. L. Merkle, J. Fluids Eng. **107**, 370 (1985).

[10]H. H. Legener, Phys. Fluids **27**, 2788 (1984).
[11]J. L. Lumley, Phys. Fluids **20**, S65 (1977), Part II.
[12]C. L. Merkle and S. Deutsch, AIAA Publ. 85-0537, 1985.
[13]G. Fortuna and T. J. Hanratty, J. Fluid Mech. **53**, 575 (1972), Part III.
[14]L. P. Purtell, P. S. Klebanoff, and F. T. Buckley, Phys. Fluids **24**, 802 (1981).
[15]N. H. Hughes, M. M. Reischman, and J. M. Holzman, in *Proceedings of the Sixth Biennial Symposium on Turbulence* (University of Missouri, Rolla, 1979), p. 274.
[16]N. K. Madavan, Ph.D. thesis, Pennsylvania State University, 1984.
[17]H. H. Legner, Bull. Am. Phys. Soc. **29**, 1514 (1984).